
**Separation Science and Technology**
Publication details, including instructions for authors and subscription information:
http://www.informaworld.com/smpp/title~content=t713708471

# Asymmetry of Peak Shapes in Linear Gas—Liquid Chromatography

Kyung Ho Row[a]; Dai-Ki Choi[b]
[a] DEPARTMENT OF CHEMICAL ENGINEERING, INHA UNIVERSITY, INCHON, KOREA [b] CFC ALTERNATIVES TECHNOLOGY CENTER KOREA INSTITUTE OF SCIENCE AND TECHNOLOGY, SEOUL, KOREA

**To cite this Article** Row, Kyung Ho and Choi, Dai-Ki(1995) 'Asymmetry of Peak Shapes in Linear Gas—Liquid Chromatography', Separation Science and Technology, 30: 19, 3615 — 3628
**To link to this Article: DOI:** 10.1080/01496399508014148
**URL:** http://dx.doi.org/10.1080/01496399508014148

SEPARATION SCIENCE AND TECHNOLOGY, **30**(19), pp. 3615–3628, 1995

# Asymmetry of Peak Shapes in Linear Gas–Liquid Chromatography

KYUNG HO ROW*
DEPARTMENT OF CHEMICAL ENGINEERING
INHA UNIVERSITY
253 YONGHYUN-DONG, NAM-KU, INCHON, KOREA

DAI-KI CHOI
CFC ALTERNATIVES TECHNOLOGY CENTER
KOREA INSTITUTE OF SCIENCE AND TECHNOLOGY
P.O. BOX 131, CHEONGRYANG, SEOUL, KOREA



## ABSTRACT

A mathematical model describing axial dispersion, interparticle mass transfer, intraparticle gas diffusion, and diffusion in a uniform thickness liquid film is used systematically to investigate the influence of intraparticle diffusivity, diffusivity in a stationary liquid phase (SLP), partition coefficient, and thickness of liquid film on the shape of the peaks in linear gas–liquid chromatography by converting Laplace transformed equations into time domain. The low diffusivities of intraparticle and/or SLP can cause the asymmetry and long tail in chromatographic peaks. A higher partition coefficient and the film thickness at low diffusivities also give skewed peaks. At a higher mass transfer rate, the peak becomes sharper. From these results a guide can be suggested to avoid the asymmetric condition of long-tailing peaks.

## INTRODUCTION

Among a variety of procedures for accurate and fast separation of mixtures, one of the most powerful and versatile separation processes is chromatography (1). In a gas–liquid chromatography, components are separated by different solubilities in the nonvolatile stationary liquid phase.

* To whom correspondence should be addressed.

The asymmetry of peak profiles is mainly caused by the nonlinear isotherm. The recent works of Guichon are particularly notable in this area, and they are well summarized in Ref. 2. However, in linear sorption this asymmetry was apparently observed and first explained by Giddings and Eyring in 1955 (3). Later, Giddings postulated the two mechanisms which might be responsible the asymmetry in gas–liquid chromatography (4). In the first, a few active sites on the solid support may lead to tailing. The second mechanism for asymmetry may originate in liquid diffusion. One empirical model widely used for the evaluation of band asymmetry is the exponentially modified Gaussian function, which is the convolution of the unit area Gaussian function and of an exponential decay of unit area (5). Many other mathematical functions have been suggested to explain the profiles of experimental peaks. The Gram–Charlier series and the Edgeworth–Cramer series were used for peaks which had a low or negligible skew (6, 7). Olive and Grimalt used the log-normal function for peaks which have low to high values of the skew (8).

Mathematical models are required to predict the elution profiles to analyze gas–liquid chromatographic systems. The peak shape of chromatography provides information about the characteristics of packings, mass transfer between the mobile phase and the stationary liquid phase (SLP), and diffusion in the SLP. The mathematical model of gas–liquid chromatography is similar to that of adsorption chromatography. A model for uniform thickness liquid film was presented by Alkarasani and McCoy (9) and further applied by Row and Lee (10–12). It included the effects of longitudinal dispersion, interparticle and intraparticle diffusion, and diffusion in the thin and uniform liquid film.

This work is limited to the asymmetry of peak profiles only in linear gas–liquid chromatography. The purpose of this work was to investigate the effects of the parameters in the mathematical model with uniform film thickness and the linear partition isotherm on the peak shape. The parameters considered were the diffusion coefficient in the pore spacing, the diffusion coefficient in the SLP, partition coefficient, the film thickness of SLP, and the interparticle mass transfer coefficient and the intraparticle mass transfer coefficient with respect to the SLP film.

## BASIC EQUATIONS

The distribution of a SLP on the solid support is seen to be very complex in the particle because of the irregularity of pore size and shape. The assumptions for establishing the governing equations of the processes are as follows (9–12):

1. The SLP is distributed uniformly on the surface of the inert solid particle.
2. The partition isotherm is linear.
3. The sorption effects for two or more solutes are considered with no interaction of the solutes.
4. Pressure drops along the column as well as any effects due to injection of the sample are ignored.
5. Adsorption effects between SLP and the surface in the particle are negligible.
6. The solid particle is assumed to be a sphere.

As the concept of uniform film thickness simplifies the phenomena of a SLP-coated porous particle, the transient material balances of a solute with three steps are

$$\frac{\partial c}{\partial t} + u\frac{\partial c}{\partial z} = \frac{E\partial^2 c}{\epsilon \partial z^2} - \frac{3}{r_p}\frac{1-\epsilon}{\epsilon} D_e \left.\frac{\partial q}{\partial r}\right|_{r=r_p} \tag{1}$$

for the mobile phase,

$$\epsilon_p \frac{\partial q}{\partial t} = D_e \frac{1}{r^2}\frac{\partial}{\partial r}\left(r^2 \frac{\partial q}{\partial r}\right) - A_p k_g \left(q - \frac{n|_{x=\delta}}{K}\right) \tag{2}$$

for the intraparticle phase, and

$$\frac{\partial n}{\partial t} = D_1 \frac{\partial^2 n}{\partial x^2} \tag{3}$$

for the SLP.

The initial and boundary conditions are:

$$c = q = n = 0 \qquad (\text{for } t = 0,\ z > 0) \tag{4}$$

$$c = c_0(t) \qquad (\text{for } t > 0,\ z = 0) \tag{5}$$

$$c = \text{finite} \qquad (\text{for } t > 0,\ z \to \infty) \tag{6}$$

$$\partial q/\partial r = 0 \qquad (\text{for } t > 0,\ r = 0) \tag{7}$$

$$\partial n/\partial x = 0 \qquad (\text{for } t > 0,\ x = 0) \tag{8}$$

$$D_e \frac{\partial q}{\partial r} = k_f(c - q) \qquad (\text{for } t > 0,\ r = r_p) \tag{9}$$

$$D_1 \frac{\partial n}{\partial x} = k_g\left(q - \frac{n}{K}\right) \qquad (\text{for } t > 0,\ x = \delta) \tag{10}$$

It is assumed that the partition effect is dominant to that of adsorption with a linear equilibrium isotherm. The solution of Eq. (1) to Eq. (10) in the Laplace domain is

$$C(s) = C_0(s) \exp\left(\frac{L}{2}\left[\frac{u_0}{E} - \left\{\left(\frac{u_0}{E}\right)^2 + 4\lambda\right\}^{1/2}\right]\right) \tag{11}$$

at the bed exit, $z = L$, where

$$\lambda = \frac{\epsilon}{E}\left(s + \frac{3(1-\epsilon)}{r_p\epsilon} k_f \left\{1 - \frac{\sinh(\lambda_2 r_p)}{r_p}\lambda_1\right\}\right) \tag{12}$$

$$\lambda_1 = \frac{r_p k_f}{D_e\lambda_2 \cosh(\lambda_2 r_p) + \left(k_f - \dfrac{D_e}{r_p}\right)\sinh(\lambda_2 r_p)} \tag{13}$$

$$\lambda_2 = \left(\frac{1}{D_e}\left[\{\epsilon_p s + A_p k_g\} - \frac{A_p k_g^2 \cosh\lambda_3}{D_e k\sqrt{\dfrac{s}{D_1}}\lambda_3 + D_e k_g \cosh\lambda_3}\right]\right)^{1/2} \tag{14}$$

$$\lambda_3 = \delta\sqrt{s/D_1} \tag{15}$$

The resulting Laplace transformed equations, Eq. (11) to Eq. (14), should be converted into the real time domain, but the analytical method is probably impossible. For an approximation technique, the equations are inverted numerically with the curve-fitting procedure suggested by Dang and Gibilaro (13). In the numerical inversion, the infinite upper integration limit is taken as the corresponding value of the frequency to amplitude ratio of the Laplace transformed equations (0.001), and it takes just about 15 seconds using a HP Vectra (Model 486/66VL) to transform the equations into the real-time domain.

## DETERMINATION OF PARAMETERS

The material used in the simulation was diethyl ether, and its boiling point is 34.6°C. The temperature throughout the column was set at 35°C, and the partition coefficient was 126.3 from the equilibrium relation $K = 0.00167 \exp(6875.0/RT)$ (14). The velocity of the carrier was fixed at 10 cm/s.

The particle size was 45/60 mesh ($r_p = 0.0136$ cm), and $A_p$ and $A_s$ were 13,000 $cm^2/cm^3$ and 27,000 $cm^2/g$, respectively (15). The interparticle porosity, $\epsilon$, was assumed to be 0.41 (16). Assuming that the SLP was

spread with a uniform film thickness, $\delta$ can be calculated as follows (16):

$$\delta = W_L/(\rho_L A_s W_s) \quad (16)$$

where $W_L$ = total weight of the SLP in the column and $W_s$ = total weight of solid particle in the column. The calculated film thickness, $\delta$, was 0.127 $\mu$m at 20% liquid loading (ratio of the weight of the SLP to that of the solid packings). Therefore, the intraparticle porosity of a SLP-coated porous particle with uniform thickness, $\epsilon_p$, can be obtained from the relationship, $\epsilon_p = \epsilon_{p'} - \delta A_p$, where $\epsilon_{p'}$ was assumed as 0.78 (12). The intraparticle porosities in the presence of the SLP, $\epsilon_p$, were 0.53, 0.39, 0.26, and 0.13 for film thicknesses of 0.2, 0.3, 0.4, and 0.5 $\mu$m, respectively.

The dependence of the fluid-film mass transfer coefficient, $k_f$, on the superficial velocity of the eluant and the particle size can be expressed by the semiempirical correlation (17)

$$k_f = D_M(1 + 0.725\mathrm{Re}^{0.50}\mathrm{Sc}^{0.33})/r_p \quad (17)$$

For the intraparticle mass transfer coefficient with respect to the SLP film, $k_g$, the correlation formula proposed by Ergun (18) was used with the assumption that it was not affected by the superficial velocity of the carrier.

$$k_g = 12.5D_M/r_p(1 - \epsilon_p/\epsilon_p) \quad (18)$$

Finally, the axial dispersion coefficient was obtained by the empirical formula (12)

$$E = 0.71D_M + r_p u_0^{1.54} \quad (19)$$

The molecular diffusivity, $D_M$, was calculated from the Chen and Othmer equation (19), and found to be 0.41 $cm^2/s$.

## RESULTS AND DISCUSSION

The effects of the parameters used in the mathematical model with the assumption of uniform film thickness, $D_e$, $D_1$, $K$, $\delta$, $K_f$, and $k_g$ (except the axial dispersion coefficient, $E$) on the shapes of the calculated concentration profiles were investigated.

### Effect of $D_e$ and $D_1$

Figure 1 shows the effect of the intraparticle diffusion coefficient, $D_e$, on the peak shapes at $D_1 = 6.5 \times 10^{-7}$ $cm^2/s$ and $K = 126.3$. $D_1$ was obtained as $6.5 \times 10^{-7}$ $cm^2/s$ from the correlation of Wilke and Chang (20). The value of $D_e$ by the parameter estimation of the frequency domain

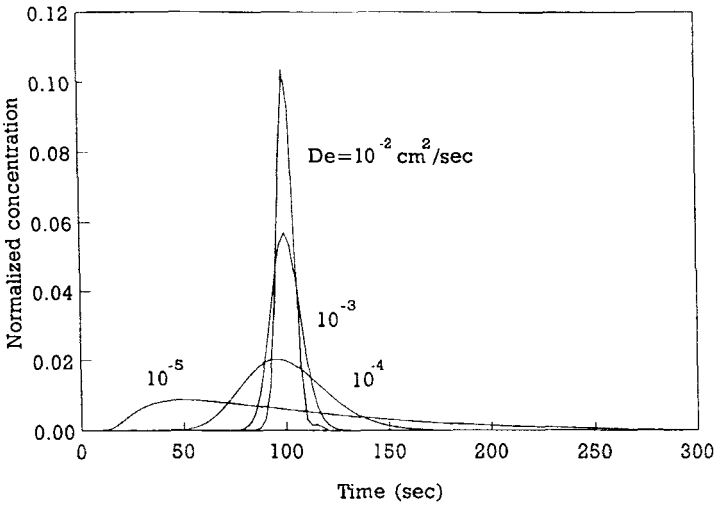


FIG. 1 Effect of $D_e$ on elution peaks ($D_1$ = 6.5 × $10^{-7}$ $cm^2/s$, $K$ = 126.3).



was $10^{-3}$ $cm^2/s$. The elution peak is symmetrical and sharp at higher intraparticle diffusivities. For a lower intraparticle diffusion, the solute needs a longer time to diffuse in and then to diffuse out, therefore the elution peaks become broader. If $D_e$ decrease further ($10^{-4}$ and $10^{-5}$ $cm^2/s$), an asymmetric chromatograph with a long peak tailing will appear. Due to the low intraparticle diffusivity, the majority of the solute does not go deeply into the porous packings and elutes after a short residence time. On the other hand, solute that diffuses into the porous packings to a greater extent requires a longer time to diffuse out, and thus a tailing band occurs.

Maintaining a intraparticle diffusivity of $10^{-3}$ $cm^2/s$ and a partition coefficient of 126.3, the asymmetry in elution profiles with a low diffusion coefficient in the SLP, $D_1$, is shown Fig. 2. At 35°C column temperature, the molecular diffusion coefficient, $D_M$, of diethyl ether was calculated to be 6.5 × $10^{-7}$ $cm^2/s$ from the Wilke and Chang equation. The overall trend of peak shapes between the two figures appears similar. Higher than $10^{-10}$ $cm^2/s$, the peak is symmetrical and sharp. But as $D_1$ decreases, the peak width becomes broader and tailing occurs. The low diffusion coefficient in the SLP renders the solute stay longer, which contributes to peak broadening, just like the behavior of the solute in a pore at low intraparticle diffusivity. The difference of several orders of magnitude

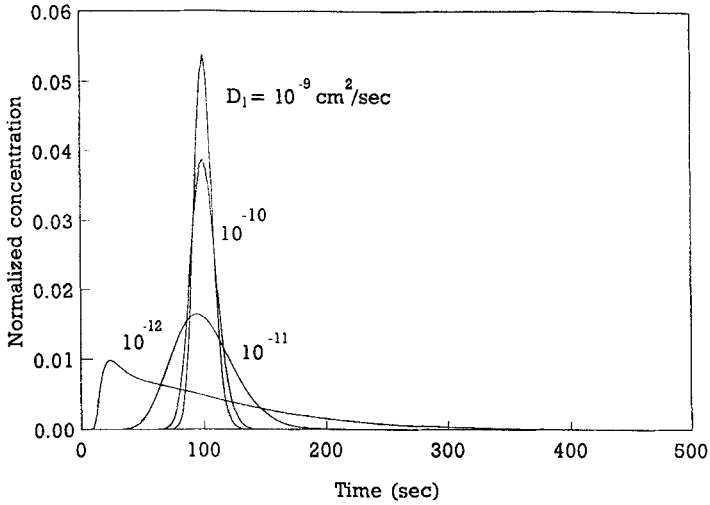


FIG. 2 Effect of $D_l$ on elution peaks ($D_e = 10^{-3}$ cm$^2$/s, $K = 126.3$).



between $D_e$ and $D_l$ is attributed to the gas and liquid states of the solute, respectively.

For low values of both $D_e$ and $D_l$, the asymmetric peak is as shown in Fig. 3. The retention times of the solute are reduced to less than 20 seconds. Another feature is very broad peak width with a long tail.

## Effect of *K*

The partition coefficient is defined by the ratio of the amount of solute per unit volume of the liquid phase to the amount of solute per unit volume of the gas phase (21). A higher partition coefficient means most of the solute is retained in the SLP. As shown in Fig. 4, the retention time and column efficiency are greatly affected by the magnitude of the partition coefficient. At $D_e = 10^{-3}$ cm$^2$/s and $D_l = 6.5 \times 10^{-7}$ cm$^2$/s, the peaks are almost symmetrical, regardless of the coefficient. However, with low intraparticle diffusivity (Fig. 5) or with a low diffusion coefficient in the SLP (Fig. 6), the lower partition coefficient shows a shorter retention time and a more asymmetric peak profile. The combined effects of a lower partition coefficient and the two diffusion coefficients considerably influence the peak shapes.

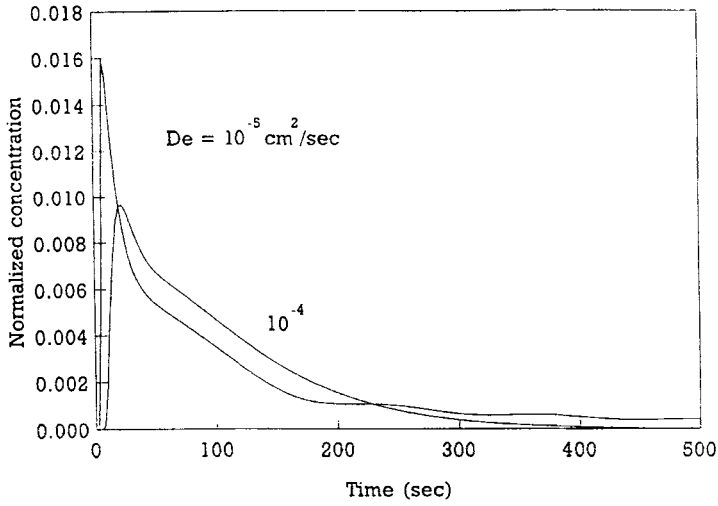


FIG. 3 Asymmetry in elution peaks at low $D_e$ and $D_i$ ($D_i = 10^{-12}$ cm$^2$/s, $K = 126.3$).

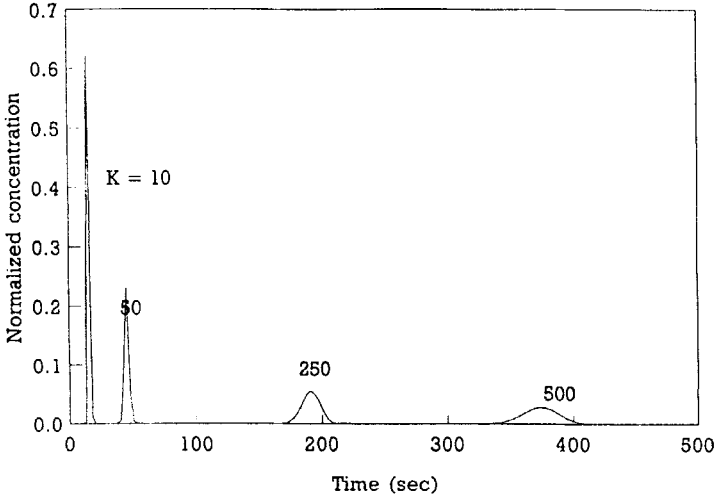


FIG. 4 Effect of $K$ on elution peaks ($D_e = 10^{-3}$, $D_i = 6.5 \times 10^{-12}$ cm$^2$/s).

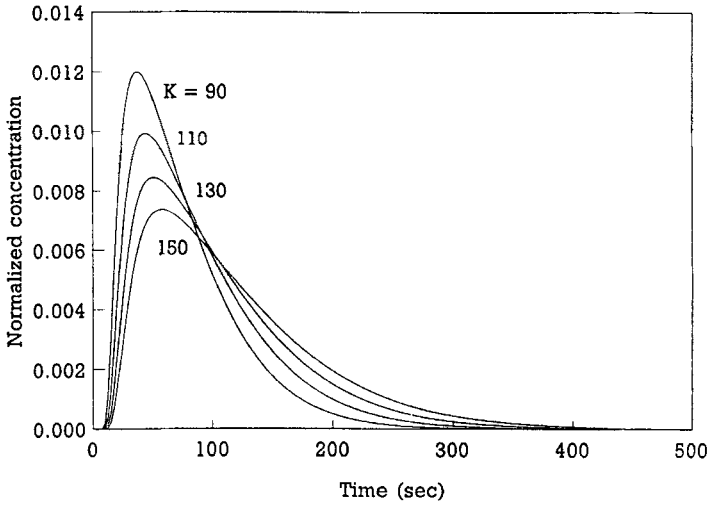


FIG. 5 Asymmetry in elution peaks with $K$ at low $D_e$ ($D_e = 10^{-6}$, $D_l = 6.5 \times 10^{-7}$ cm$^2$/s).

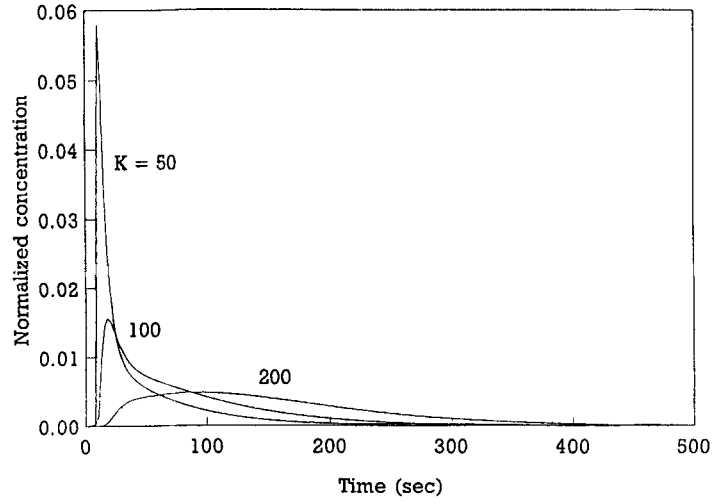


FIG. 6 Asymmetry in elution peaks with $K$ at low $D_l$ ($D_e = 10^{-3}$, $D_l = 6.5 \times 10^{-12}$ cm$^2$/s).

## Effect of δ

Contrary to the adsorption characteristics in the partition system, the mixtures to be separated are partitioned preferentially by a SLP supported on a relatively inert surface of porous particle. Separation in the partition system is mainly affected by the different solubilities in the SLP. One of the main advantages of the partition system over adsorption is that it has very versatile liquid phases. The inner part of the porous solid packing in gas–liquid chromatography consists of solid packing, SLP, and pore spacing. At a thicker film thickness, δ, the solute takes a longer time to diffuse into the SLP and out of the packings, so its peak shape shows longer retention times and tails (Fig. 7). At low intraparticle diffusivity, the peak shape of the thinner film shows a shorter retention time and more asymmetry (Fig. 8). It may be said that the elution time is highly dependent on the film thickness of the SLP. At 0.5 μm, it increases to almost 1800 seconds.

## Effect of $K_f$ and $k_g$

Sensitivity analyses of the response curves with respect to $k_f$ and $k_g$ give useful indications of how these parameters influence the peak shape. At $D_e = 10^{-3}$ and $D_l = 6.5 \times 10^{-7}$ cm²/s, the effect of interparticle film resistance on the response curve is as illustrated in Fig. 9, from which it

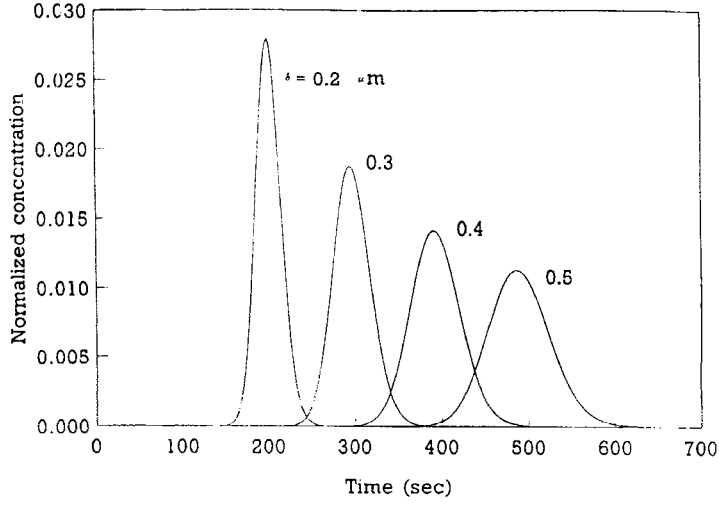


FIG. 7 Effect of δ on elution peaks ($D_e = 10^{-3}$, $D_l = 6.5 \times 10^{-7}$ cm²/s, $K = 126.3$).

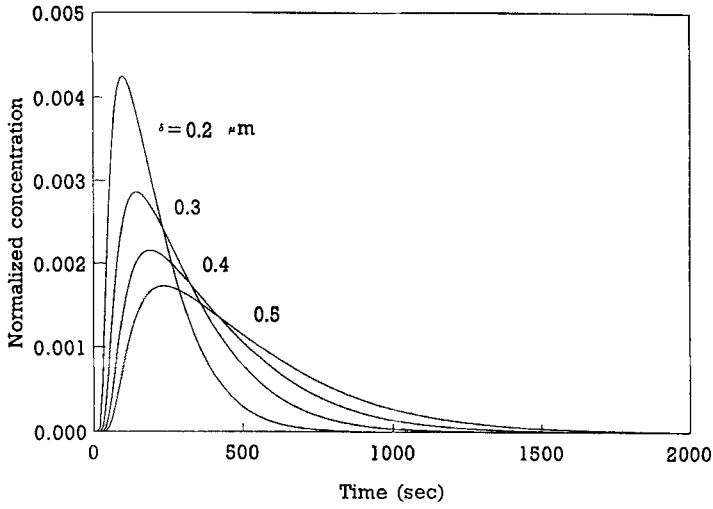


FIG. 8 Asymmetry in elution peaks with δ at low $D_e$ ($D_e = 10^{-6}$, $D_1 = 6.5 \times 10^{-7}$ cm²/s, $K = 126.3$).

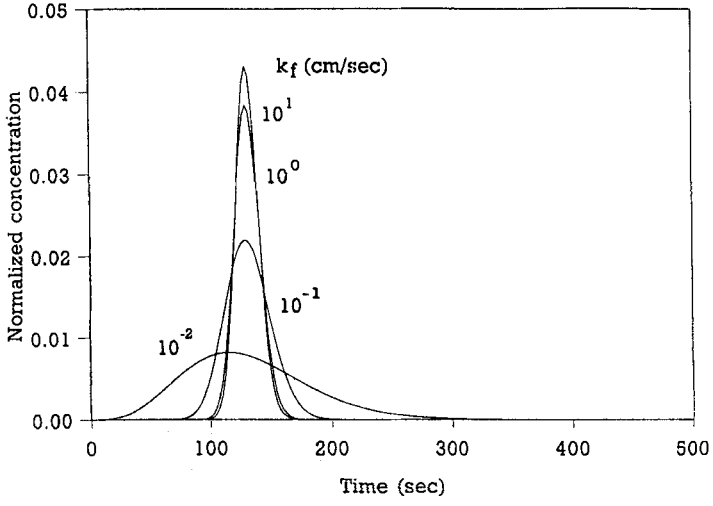


FIG. 9 Dependence of the peak on $k_f$ ($D_e = 10^{-3}$, $D_1 = 6.5 \times 10^{-7}$ cm²/s, $K = 126.3$).

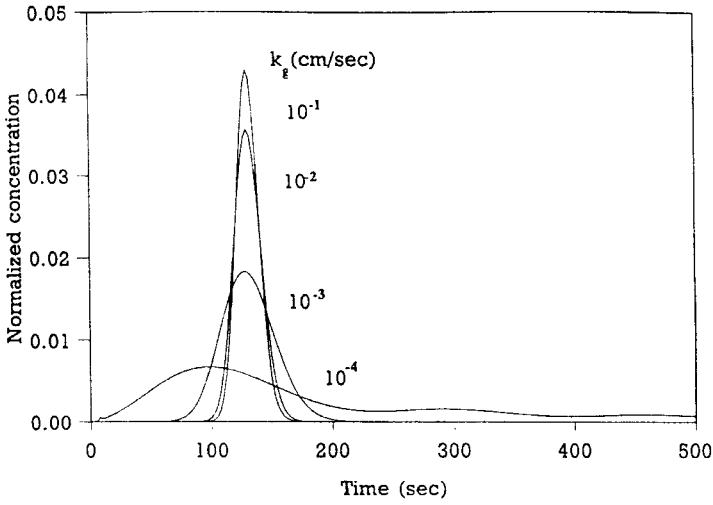


FIG. 10 Dependence of the peak on $k_g$ ($D_e = 10^{-3}$, $D_1 = 6.5 \times 10^{-7}$ cm$^2$/s, $K = 126.3$).



is found that the effect is not influenced when the coefficient is greater than 10.0 cm/s. The interparticle mass transfer coefficient calculated from the correlation of Eq. (17) is 14.57 cm/s.

Figure 10 shows the effect of intraparticle mass transfer film resistance on the peak shape with the same $D_e$ and $D_1$ as in Fig. 9; a decrease in the coefficient, $k_g$, gives rise to a progressively broader peak. However, when the coefficient is greater than $10^{-1}$ cm/s, the peak shape is almost the same. The intraparticle mass transfer coefficient from the correlation of Eq. (18) is 44.84 cm/s. The shape of the peak is almost the same and looks similar as $k_g$ approaches infinity. It was shown by moment analysis that the interparticle and intraparticle film resistances to the second moment of the frequency response are linearly additive (9). The second moment expresses the variance of an elution peak and is a measure of band broadening. At a higher mass transfer rate, the peak becomes sharper.

## NOTATION

| | |
|---|---|
| $A_p$ | surface area of porous particle per unit volume (cm$^3$/cm$^3$) |
| $A_s$ | surface area of porous particle per unit mass (cm$^2$/g) |
| $c$ | concentration of solute in mobile phase (gmol/cm$^3$) |
| $c_0$ | inlet concentration of solute (gmol/cm$^3$) |
| $C(s)$ | Laplace transform of $c(t)$ |

$D_e$ diffusion coefficient in the pore spacing ($cm^2/s$)
$D_l$ diffusion coefficient in the SLP ($cm^2/s$)
$D_M$ molecular diffusivity ($cm^2/s$)
$E$ axial dispersion coefficient ($cm^2/s$)
$k_f$ interparticle mass transfer coefficient (cm/s)
$k_g$ intraparticle mass transfer coefficient with respect to SLP film (cm/s)
$K$ partition coefficient
$L$ column length in partition section and desorption section (cm)
$n$ concentration of solute in stationary liquid phase ($gmol/cm^3$)
$q$ concentration of solute in pore spacing ($gmol/cm^3$)
$r$ radial distance (cm)
Re Reynolds number
$r_p$ radius of porous particle (cm)
$s$ variable of Laplace transform
Sc Schmidt number
SLP stationary liquid phase
$t$ time (second)
$T$ column temperature (K)
$u$ interstitial velocity of carrier gas (cm/s)
$u_0$ superficial velocity of carrier gas or desorbent (cm/s)
$W_L$ total weight of SLP in the column (g)
$W_s$ total weight of solid particle in the column (g)
$x$ distance perpendicular to surface of porous particle (cm)
$z$ axial distance (cm)



### *Greek Letters*

$\lambda$, $\lambda_1$, $\lambda_2$, $\lambda_3$ values defined by Eq. (12) to Eq. (15)
$\delta$ film thickness of SLP ($\mu m$)
$\epsilon$ void fraction of chromatographic column
$\epsilon_p$ intraparticle porosity with presence of SLP
$\epsilon_{p'}$ intraparticle porosity with the uncoated porous particle
$\rho_L$ density of SLP ($g/cm^3$)

## ACKNOWLEDGMENTS

K.H.R. gratefully acknowledges the helpful comments of Prof. J. C. Giddings and the financial support of INHA University for Fiscal Year 1995.

## REFERENCES


1. C. J. King, *Separation Processes*, 2nd ed., McGraw-Hill, New York, 1980.
2. G. Guichon, S. Golshan-Shirazi, and A. M. Katti, *Fundamentals of Preparative and Nonlinear Chromatography*, Academic Press, Boston, 1994.
3. J. C. Giddings and H. Eyring, *J. Phy. Chem.*, *59*, 416 (1955).
4. J. C. Giddings, *Anal. Chem.*, *35*, 1999 (1963).
5. D. Hanggi and P. W. Carr, *Ibid.*, *57*, 2394 (1985).
6. F. Dondi and F. Pulidori, *J. Chromatogr.*, *284*, 293 (1984).
7. J. Grimalt, H. Iturriaga, and J. O. Olive, *Anal. Chim. Acta*, *201*, 193 (1987).
8. J. Olive and J. O. Grimalt, *J. Chromatogr. Sci.*, *29*, 70 (1991).
9. M. A. Alkarasani and B. J. McCoy, *Chem. Eng. J.*, *23*, 81 (1982).
10. K. H. Row, Ph.D. Thesis, Korea Advanced Institute of Science & Technology, Seoul, 1986.
11. K. H. Row and W. K. Lee, *Korean J. Chem. Eng.*, *3*, 7 (1986).
12. K. H. Row and W. K. Lee, *J. Chem. Eng. Jpn.*, *19*, 173 (1986).
13. N. D. P. Dang and L. G. Gibilaro, *Chem. Eng. J.*, *8*, 157 (1974).
14. I. Moon, K. H. Row, and W. K. Lee, *Korean J. Chem. Eng.*, *2*, 155 (1985).
15. *Chromosorb Diatomite Supports for Gas–Liquid Chromatography*, Johns-Manville, 1984.
16. S. D. Nogare and R. S. Juvet, *Gas–Liquid Chromatography, Theory and Practice*, Wiley, New York, 1962.
17. S. C. Foo and R. G. Rice, *AIChE J.*, *21*, 16 (1975).
18. S. Ergun, *Chem. Eng. Prog.*, *48*, 227 (1952).
19. N. H. Chen and D. F. Othmer, *J. Chem. Eng. Data*, *7*, 37 (1962).
20. C. R. Wilke and P. Chang, *AIChE J.*, *1*, 264 (1955).
21. H. M. McNair and A. J. P. Bonelli, *Basic Gas Chromatography*, Varian Aerograph, Berkeley, 1969.


*Received by editor August 22, 1994*
*Revision received April 25, 1995*